# Accepted Manuscript

Size selection of dispersed, exfoliated graphene flakes by controlled centrifugation

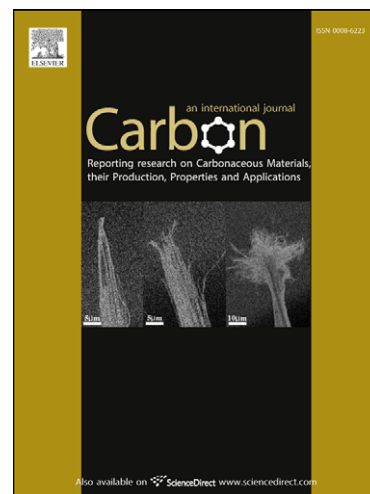Umar Khan, Arlene O'Neill, Harshit Porwal, Peter May, Khalid Nawaz, Jonathan N. Coleman

Please cite this article as: Khan, U., O'Neill, A., Porwal, H., May, P., Nawaz, K., Coleman, J.N., Size selection of dispersed, exfoliated graphene flakes by controlled centrifugation, *Carbon* (2011), doi: 10.1016/j.carbon. 2011.09.001

Size selection of dispersed, exfoliated graphene flakes by controlled centrifugation

Umar Khan[1], Arlene O'Neill[1], Harshit Porwal[1], Peter May[1], Khalid Nawaz[2] and Jonathan N Coleman[1]*

[1]School of Physics and CRANN, Trinity College Dublin, Dublin 2, Ireland

[2]School of Chemical and Materials Engineering, NUST, H-12 Islamabad, Pakistan

*Corresponding author. Tel +353 1 8963859. Email address: colemaj@tcd.ie (J.N. Coleman)

Abstract: Liquid exfoliation of graphene generally results in flakes with lateral size of one micron or less on average, too small for many applications. In this paper we describe a method to separate an existing dispersion with mean flake length of ~1 μm into fractions, each with different mean flake size. The initial dispersion is centrifuged at a high centrifugation rate, separating small flakes in the supernatant from large flakes in the sediment. Redispersion of the sediment, followed by successive centrifugation, separation and redispersion cycles can be used to separate the flakes by size so long as the centrifugation rate is decreased with each cycle. This procedure results in a range of dispersions with mean flake length varying from 1 μm for the highest final centrifugation rate to 3.5 μm for the sample whose final centrifugation rate was 500 rpm.

1. Introduction

Liquid phase exfoliation of graphite to give graphene has received a lot of attention in recent years.[1] Such processes take graphite as a starting material and exfoliate it down to thin flakes dispersed as a colloidal suspension, usually in a solvent. A number of types of exfoliation process exist with two examples being oxidation of graphite to give graphene oxide (GO)[2-6] and sonication-assisted exfoliation of graphite followed by stabilisation

1

using special solvents or surfactants/stabilisers.[7-26] One advantage of GO based dispersion is that the flakes tend to be predominately monolayers. However, the oxidisation process tends to introduce large quantities of structural defects which shift the physical properties away from pristine graphene. Solvent or surfactant exfoliated graphene gives defect-free flakes but with relatively low monolayer content. Each method results in dispersions with concentrations of up to a few mg/ml produced in up to litre batches.[1]

For many applications, solvent or surfactant stabilised graphene is attractive due to its defect free nature. However this method has one very serious weakness; it tends to produce small flakes with typical flake size of ~1 micron. This is a significant problem. Liquid exfoliation of graphene is usually sold as a method to produce graphene in large quantities for applications such as in composites or films. However, many of these applications require flakes which are considerably larger than those currently available. For example, Gong et al recently showed that in order to produce effectively reinforced graphene-polymethylmethacrylate composites, the flake length would have to be a few microns or greater.[27] Currently available exfoliated graphene is usually significantly smaller than this which partly explains why most graphene composite papers describe reinforcement values much lower than the theoretical limit[28] of $dY/dV_f \sim 1$ TPa where Y is the composite modulus and $V_f$ is the graphene volume fraction.[29-38] Alternatively, conducting graphene networks have been mooted as potential transparent electrodes or supercapacitor electrodes. However, the conductivity of such networks is limited by interflake junctions.[39] Smaller flakes result in more junctions and so lower conductivity.[40] Thus, there is a real need to increase the size of dispersed flakes. Ideally, we would tune the dispersion/exfoliation process to give larger flakes. However, while some progress has been made in this area, it is worth exploring methods to post-treat existing dispersions to select flakes by size. While a number of methods have been demonstrated to separate GO flasks by lateral size,[41-43] to

our knowledge, lateral size selection has not been demonstrated for defect free graphene. Here, we describe a method to take an existing dispersion of graphene in a solvent and separate flakes by size using controlled centrifugation. We have produced a set of dispersions with mean flake lengths varying from 1 to 3.5 microns. This method is versatile and could easily be applied to surfactant stabilised graphene[19, 20, 22] or indeed any exfoliated layered compounds.[44]

## 2. Experimental section

Graphite flakes and the solvent N-methyl pyrrolidone (NMP) were purchased from Sigma Aldrich. Bath sonication was performed using a Branson1510E-MT while tip sonication was applied with a GEX600, 48 W, 24 kHz, flat head probe. Centrifugation (CF) was carried out using a Hettich Mikro 22R for 45 minutes in all cases. Supernatant was separated from sediment by removing the top 80% of the dispersion by pipette. Optical absorbance measurements were performed using a Varian Cary 6000i. TEM measurements were made on samples prepared by drop casting a few drops of dispersion on to a holey carbon grid using a Joel 2100. Thin films for Raman analysis were prepared by vacuum filtration of the dispersion through a porous membrane (PVDF, pore size 0.02 µm). Raman measurements were performed with a 633nm, Horiba Jobin Yvon LabRAM- HR.

## 3. Results and Discussion

While liquid exfoliation generally results in flakes which are small on average, the flake size distribution can be quite broad. In this paper, we will develop methods to post-treat dispersions of exfoliated graphene to predominately select flakes from the upper end of the distribution. However, to achieve this, we first need to determine the baseline flake size distribution achieved using standard dispersion techniques. To do this we sonicated graphite

3

powder (1.65g) in 500ml of NMP in a sonic bath for 168 hrs. This was then centrifuged at 500 rpm for 45 minutes and the top 80% of the supernatant pipetted off. The concentration of the supernatant was measured by optical absorption to be 0.45 mg/ml.[18] TEM analysis showed the supernatant to be rich in multilayer graphene flakes with a typical example shown in figure 1A. From the TEM images, we measured the long dimension (the length, L) for ~90 flakes. In addition, we estimated the flake thickness (i.e. the number of stacked monolayers per flake, N) using the edge counting method.[18] These data are summarised in the histograms in figure 1B&C. The flake length varied from ~150 nm to ~4μm (mean 1.1 μm), while the flake thickness varied from 1 to 6 monolayers (mean 2.8). In the authors' experience, this is typical of what is found for sonicated solvent-exfoliated graphene.[16-18, 21] However, it is important to point out that these are not absolute limits simply because such a small sample is extremely unlikely to contain the largest and smallest flakes in the distribution. Thus, small populations of flakes outside these limits probably exist although we did not observe them during our statistical analysis. In addition Raman analysis of a film prepared by vacuum filtration of this dispersion gave a spectrum typical of graphene. The D/G band ratio was larger than that of the starting powder by ~0.2, a result which is consistent with small defect-free flakes.[18, 20, 21]
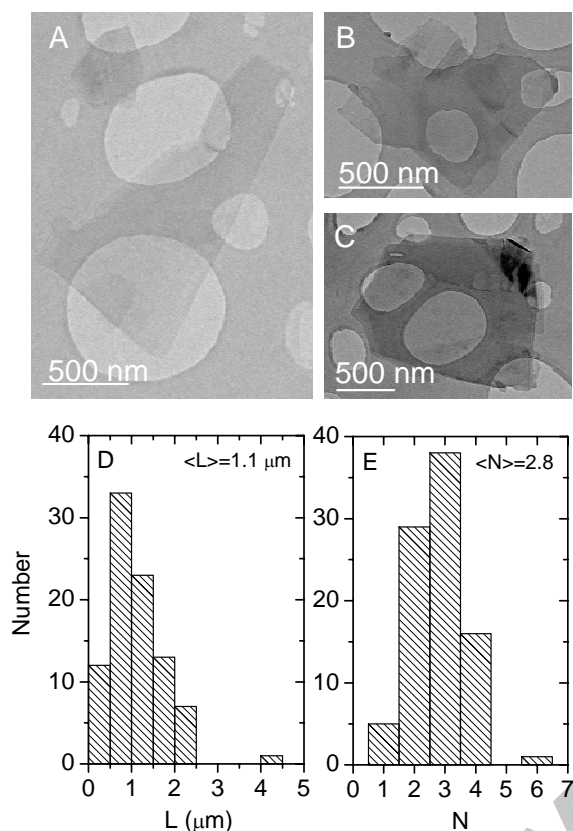
*Fig 1: Exfoliated graphene prepared by bath sonication and centrifugation at 500 rpm without size selection. A-C) TEM images of typical exfoliated flakes. Histrograms of D) flake lengths, L, and E) flake thicknesses. Flake thickness is expressed as the number of stacked monolayers per flakes, N.*

While size selection could easily be achieved by chromatography,[45] this method usually gives limited quantities of size selected material. Thus, for practical reasons, we chose to adopt controlled centrifugation. Recently, we reported that that for centrifuged graphene dispersions, the average lateral flake size decreases as the centrifugation rate (rpm) is increased.[18, 20] This means that centrifugation at a high rate results in the separation of small flakes which remain dispersed from large flakes which sediment out. The sediment can be redispersed resulting in the flakes being separated by size into two different dispersions. We note that dispersions of sonicated graphite always contain some unexfoliated graphitic

crystallites.[17] These must be removed by a centrifugation step with 500 rpm usually enough to remove the graphitic crystallites while leaving the flakes dispersed. Thus, when redispersing the sediment it is always necessary to centrifuge. However, one can choose the centrifugation rate. If one chooses 500 rpm to remove only the crystallites, the result will be the initial supernatant with only small flakes, the redispersed centrifuged sediment with all other flake sizes and a second sediment containing the crystallites. However, one could choose a higher centrifugation rate for the redispersed sediment. This would remove crystallites and the largest flakes leaving only medium size flakes dispersed. In this case, the result will be the initial supernatant with only small flakes, the redispersed, centrifuged sediment with medium sized flakes and a second sediment with large flakes and crystallites. This suggests that controlled centrifugation can potentially act as a size selection mechanism.
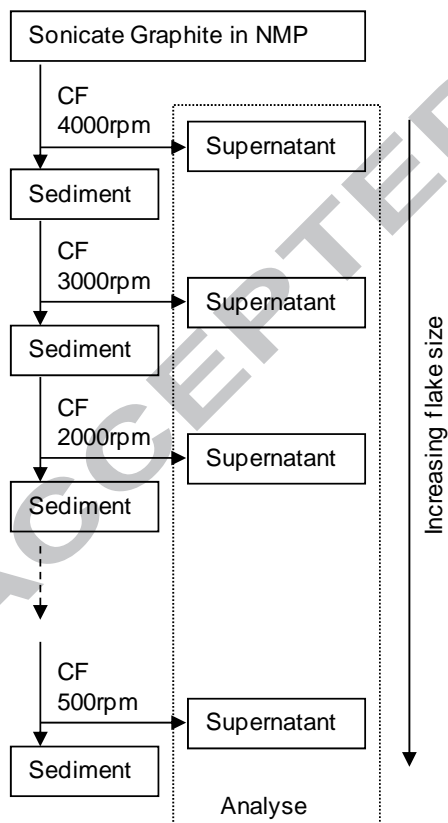


*Figure 2: Schematic showing separation process.*

To test this, we designed a centrifugation-based, size selection procedure as summarised in figure 2. Basically, we prepared a dispersion as described above and centrifuged at 4000 rpm. The supernatant was set aside and the sediment redispersed in 16ml NMP by bath sonication for 15 minutes. This redispersed sediment was then centrifuged at 3000 rpm, the supernatant was set aside and the sediment again redispersed in 16ml NMP. This procedure was repeated a further four times, centrifuging the redispersed sediment at 2000, 1000, 700 and 500 rpm, each time collecting the supernatant. After the 500 rpm centrifugation, the procedure was stopped as we have found 500 rpm to be the minimum required to remove unexfolaited graphitic crystallites. Each of the supernatants were then analysed by absorption spectroscopy to measure the dispersed concentration. In addition, the supernatants were vacuum filtered to form thin films which were analysed by Raman spectroscopy. Finally, three of the supernatants (3000, 1000 and 500 rpm) were characterised by TEM and the flake size, L and thickness, N, measured.

It is worth noting that to achieve a range of size separated samples, it is necessary to centrifuge with successively lower rates. If the procedure is attempted with the same centrifugation rate at each step, the same flake size will be achieved in all supernatants (see SI). In addition, we repeated exactly the same procedure but for tip sonicated (rather than bath sonicated) dispersions. These results are also shown in the SI.
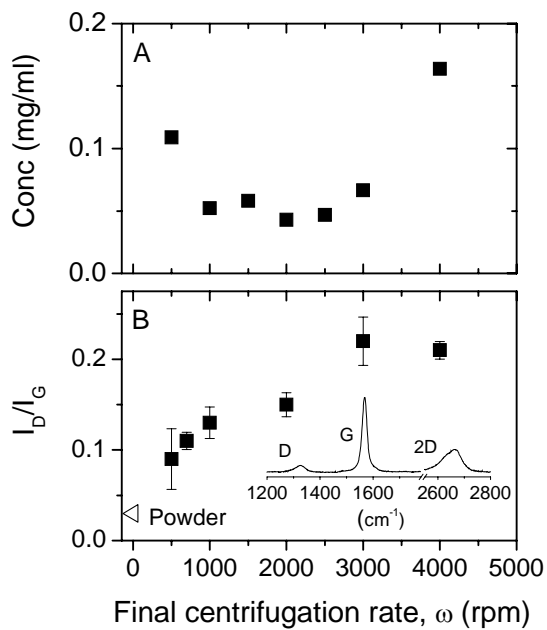
*Figure 3: A) Dispersed concentration measured by absorption spectroscopy as a function of final centrifugation rate. B) Ratio of Raman D:G bands measured on films prepared from size selected dispersions as a function of final centrifugation rate. Inset: Raman spectra for the film of size selected flakes prepared after a final centrifugation at 500 rpm.*

8
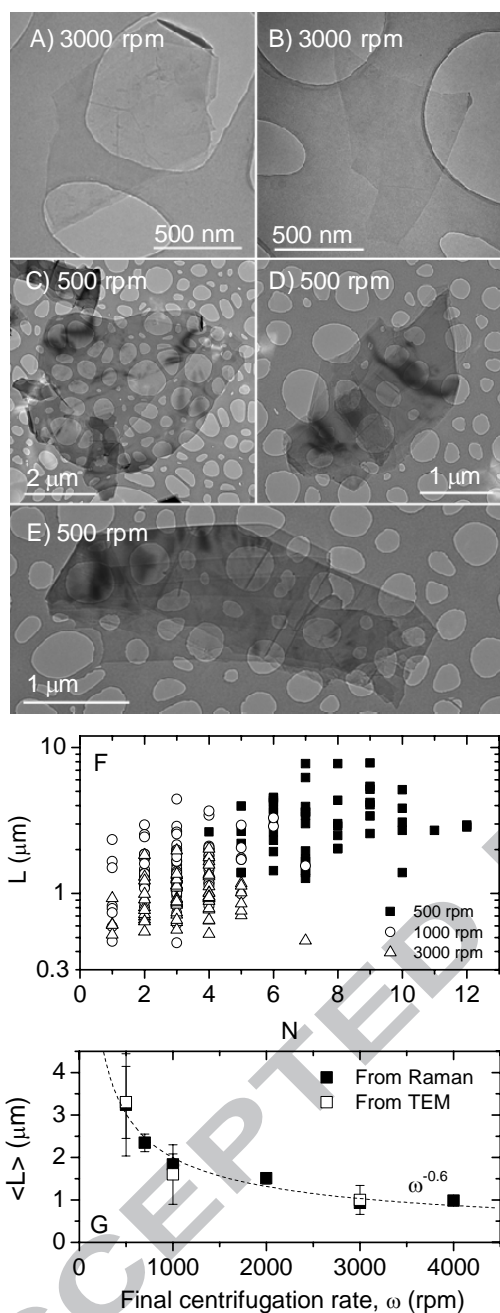
*Figure 4*

*TEM images of flakes prepared by the scheme in figure 2 with a final centrifugation rate of A*

*& B) 3000 rpm and C-E) 500 rpm. F) Individual flake length plotted versus estimated flake*

*thickness (number of monolayers, N) for dispersions with final centrifugation rates of 500,*

*1000 and 3000 rpm. G) Mean flake length as measured from TEM and as estimated from*

*both Raman. The dashed line indicates an empirical scaling behaviour of $\omega^{-0.6}$.*

9

Shown in figure 3A are the dispersed concentrations as a function of the centrifugation rate of the final centrifuge experienced by the sample. The concentration falls from a high value of ~0.17 mg/ml for the 4000 rpm sample to a constant value of ~0.05 mg/ml. The final sample, centrifuged for the last time at 500 rpm displayed a slightly higher concentration of ~0.1 mg/ml.

Of more interest is the Raman data. A typical Raman spectrum measured on a film prepared from the sample whose final CF rate was 500 rpm is shown in the inset of figure 3B (the complete set of spectra are shown in figure S2). These spectra have the D, G and 2D bands typical of graphitic material. Of interest here is the ratio of the intensities of the D and G bands, $I_D/I_G$. This ratio decreases from ~0.22 to ~0.08 as the final CF rate is decreased from 4000 to 500 rpm. For solvent exfoliated graphene flakes, this band is thought to be associated with the presence of flake edges and so is linked to the flake length by

$$I_D/I_G - (I_D/I_G)_{Powder} = k/L \qquad (1)$$

where k is a constant.[18, 21] Thus the decrease in $I_D/I_G$ with decreasing rpm is a manifestation of increasing flake size. (N.B. This expression is not to be confused with that of Cancado et al which describes basal plane defects.)[46]

We can confirm the increase in flake length with decreasing (final) rpm by TEM analysis of the 3000, 1000 and 500 rpm samples. Shown in figures 4 A-E are typical TEM images for the 3000 and 500 rpm samples. It is immediately clear from the images that the 3000 rpm flakes are much smaller than the 500 rpm ones. To confirm this, we measured the individual flake length, L, and the individual flake thicknesses, N, for ~50-100 flakes for each CF rate as shown in figure 4D (see also figure S3). It is clear from this data that L increases as the final CF rate decreases. We measured mean values of L to be 3.3, 1.6 and 0.94 μm for the 500, 1000 and 3000 rpm samples as shown in figure 4G. We can use this

data, in combination with the Raman data, to estimate k (in equation 1) by plotting $I_D/I_G$ versus $1/<L>$ (figure S4). This gives a value of k=0.17±0.05, slightly different to the previously found value of 0.26.[18, 21] This fit also gave use $(I_D/I_G)_{powder}$=0.037 in good agreement with the measured value of 0.03. We can now use equation 1 to estimate the flake length from the Raman data as shown in figure 4G. This data shows a continuous increase from ~1 μm for the 4000 rpm sample to ~3.5 μm for the 500 rpm sample. We note that empirically, the flake length scales with final CF rate as $\omega^{-0.6}$.

While the mean values of N were 3.2 and 3.0 respectively for the 3000 and 1000 samples, similar to the normal dispersion, $<N>$ was 7.3 for the 500 rpm sample, considerably larger. This means that the flake aspect ratio (here defined as length/thickness i.e. L/(N×0.35nm)) does not necessarily increase monotonically with final CF rate. In fact the measured aspect ratios were 990, 1680, 1310, 1180 for the 3000 rpm, 1000 rpm, 500 rpm and normally dispersed samples respectively. In spite of the slightly increased thickness of the 500 rpm flakes, their increased length will be advantageous for a range of applications from mechanical composites[27] to conducting thin films[47]. Their thickness varied in the range 6≤N≤12 while their length varied in the range 1.2 μm≤N≤7.8 μm. We note that the smallest flake observed in this sample was larger than the mean for the normal dispersion. In addition, we note that it should be possible to use this size-selected sample as a starting point for further centrifugation-based treatment in order to refine the sample and narrow the length distribution.

4. Conclusions

We have demonstrated that controlled centrifugation can be used to separate graphene flakes by size. Centrifugation at high rates results in small flakes being dispersed but larger ones sedimenting out. This sediment can be collected and redispersed. Centrifugation at a

11

lower rate then results in a dispersion of slightly larger flakes and the rejection of the rest. Repeating this procedure a number of times results in the separation of the original dispersion into a number of fractions each with different mean flake length, in this case from ~1 to ~3.5 µm. Although we have demonstrated this procedure for solvent exfoliated graphene, it could easily be extended to surfactant exfoliated graphene or indeed otherexfoliated layered compounds.

[1]      Park S, Ruoff RS. Chemical methods for the production of graphenes. Nature Nanotechnology. 2009;4(4):217-24.

[2]      Park S, An JH, Jung IW, Piner RD, An SJ, Li XS, et al. Colloidal Suspensions of Highly Reduced Graphene Oxide in a Wide Variety of Organic Solvents. Nano Letters. 2009;9(4):1593-7.

[3]      Park S, An JH, Piner RD, Jung I, Yang DX, Velamakanni A, et al. Aqueous Suspension and Characterization of Chemically Modified Graphene Sheets. Chemistry of Materials. 2008;20(21):6592-4.

[4]      Stankovich S, Dikin DA, Dommett GHB, Kohlhaas KM, Zimney EJ, Stach EA, et al. Graphene-based composite materials. Nature. 2006;442(7100):282-6.

[5]     Stankovich S, Dikin DA, Piner RD, Kohlhaas KA, Kleinhammes A, Jia Y, et al. Synthesis of graphene-based nanosheets via chemical reduction of exfoliated graphite oxide. Carbon. 2007;45(7):1558-65.

[6]     Stankovich S, Piner RD, Chen XQ, Wu NQ, Nguyen ST, Ruoff RS. Stable aqueous dispersions of graphitic nanoplatelets via the reduction of exfoliated graphite oxide in the presence of poly(sodium 4-styrenesulfonate). Journal of Materials Chemistry. 2006;16(2):155-8.

[7]     Blake P, Brimicombe PD, Nair RR, Booth TJ, Jiang D, Schedin F, et al. Graphene-based liquid crystal device. Nano Letters. 2008;8(6):1704-8.

[8]     Bourlinos AB, Georgakilas V, Zboril R, Steriotis TA, Stubos AK. Liquid-Phase Exfoliation of Graphite Towards Solubilized Graphenes. Small. 2009;5(16):1841-5.

[9]     Bourlinos AB, Georgakilas V, Zboril R, Steriotis TA, Stubos AK, Trapalis C. Aqueous-phase exfoliation of graphite in the presence of polyvinylpyrrolidone for the production of water-soluble graphenes. Solid State Commun. 2009;149(47-48):2172-6.

[10]    Coleman JN. Liquid-Phase Exfoliation of Nanotubes and Graphene. Advanced Functional Materials. 2009;19(23):3680-95.

[11]    De S, King PJ, Lotya M, O'Neill A, Doherty EM, Hernandez Y, et al. Flexible, Transparent, Conducting Films of Randomly Stacked Graphene from Surfactant-Stabilized, Oxide-Free Graphene Dispersions. Small. 2009;6 (3):458-64.

[12]    Green AA, Hersam MC. Solution Phase Production of Graphene with Controlled Thickness via Density Differentiation. Nano Letters. 2009;9(12):4031-6.

[13]    Hamilton CE, Lomeda JR, Sun ZZ, Tour JM, Barron AR. High-Yield Organic Dispersions of Unfunctionalized Graphene. Nano Letters. 2009;9(10):3460-2.

[14]    Hao R, Qian W, Zhang LH, Hou YL. Aqueous dispersions of TCNQ-anion-stabilized graphene sheets. Chemical Communications. 2008;48):6576-8.

[15]    Hasan T, Torrisi F, Sun Z, Popa D, Nicolosi V, Privitera G, et al. Solution-phase exfoliation of graphite for ultrafast photonics. Physica Status Solidi B-Basic Solid State Physics. 2010;247(11-12):2953-7.

[16]    Hernandez Y, Lotya M, Rickard D, Bergin SD, Coleman JN. Measurement of Multicomponent Solubility Parameters for Graphene Facilitates Solvent Discovery. Langmuir. 2010;26(5):3208-13.

[17]    Hernandez Y, Nicolosi V, Lotya M, Blighe FM, Sun ZY, De S, et al. High-yield production of graphene by liquid-phase exfoliation of graphite. Nature Nanotechnology. 2008;3(9):563-8.

[18]    Khan U, O'Neill A, Lotya M, De S, Coleman JN. High-Concentration Solvent Exfoliation of Graphene. Small. 2010;6(7):864-71.

[19]    Lotya M, Hernandez Y, King PJ, Smith RJ, Nicolosi V, Karlsson LS, et al. Liquid Phase Production of Graphene by Exfoliation of Graphite in Surfactant/Water Solutions. Journal of the American Chemical Society. 2009;131(10):3611-20.

[20]    Lotya M, King PJ, Khan U, De S, Coleman JN. High-Concentration, Surfactant-Stabilized Graphene Dispersions. ACS Nano. 2010;4(6):3155-62.

[21]    O'Neill A, Khan U, Nirmalraj PN, Boland JJ, Coleman JN. Graphene Dispersion and Exfoliation in Low Boiling Point Solvents. The Journal of Physical Chemistry C. 2011;115(13):5422-8.

[22]    Smith RJ, Lotya M, Coleman JN. The importance of repulsive potential barriers for the dispersion of graphene using surfactants. New Journal of Physics. 2010;12:125008.

[23]    Vadukumpully S, Paul J, Valiyaveettil S. Cationic surfactant mediated exfoliation of graphite into graphene flakes. Carbon. 2009;47(14):3288-94.

[24]    Alzari V, Nuvoli D, Scognamillo S, Piccinini M, Gioffredi E, Malucelli G, et al. Graphene-containing thermoresponsive nanocomposite hydrogels of poly(N-

isopropylacrylamide) prepared by frontal polymerization. Journal of Materials Chemistry. 2011;21(24):8727-33.

[25]    Catheline A, Valles C, Drummond C, Ortolani L, Morandi V, Marcaccio M, et al. Graphene solutions. Chemical Communications. 2011;47(19):5470-2.

[26]    Nuvoli D, Valentini L, Alzari V, Scognamillo S, Bon SB, Piccinini M, et al. High concentration few-layer graphene sheets obtained by liquid phase exfoliation of graphite in ionic liquid. Journal of Materials Chemistry. 2011;21(10):3428-31.

[27]    Gong L, Kinloch IA, Young RJ, Riaz I, Jalil R, Novoselov KS. Interfacial Stress Transfer in a Graphene Monolayer Nanocomposite. Advanced Materials. 2010;22(24):2694-7.

[28]    Padawer GE, Beecher N. On Strength and Stiffness of Planar Reinforced Plastic Resins. Polymer Engineering and Science. 1970;10(3):185-92.

[29]    Hu HW, Chen GH. Electrochemically Modified Graphite Nanosheets and Their Nanocomposite Films with Poly(vinyl alcohol). Polymer Composites. 2010;31(10):1770-5.

[30]    Jiang L, Shen XP, Wu JL, Shen KC. Preparation and Characterization of Graphene/Poly(vinyl alcohol) Nanocomposites. Journal of Applied Polymer Science. 2010;118(1):275-9.

[31]    Kim IH, Jeong YG. Polylactide/Exfoliated Graphite Nanocomposites with Enhanced Thermal Stability, Mechanical Modulus, and Electrical Conductivity. Journal of Polymer Science Part B-Polymer Physics. 2010;48(8):850-8.

[32]    Liang JJ, Huang Y, Zhang L, Wang Y, Ma YF, Guo TY, et al. Molecular-Level Dispersion of Graphene into Poly(vinyl alcohol) and Effective Reinforcement of their Nanocomposites. Advanced Functional Materials. 2009;19(14):2297-302.

15

[33]     Miller SG, Bauer JL, Maryanski MJ, Heimann PJ, Barlow JP, Gosau JM, et al. Characterization of epoxy functionalized graphite nanoparticles and the physical properties of epoxy matrix nanocomposites. Composites Science and Technology. 2010;70(7):1120-5.

[34]     Putz KW, Compton OC, Palmeri MJ, Nguyen ST, Brinson LC. High-Nanofiller-Content Graphene Oxide-Polymer Nanocomposites via Vacuum-Assisted Self-Assembly. Advanced Functional Materials. 2010;20(19):3322-9.

[35]     Ramanathan T, Abdala AA, Stankovich S, Dikin DA, Herrera-Alonso M, Piner RD, et al. Functionalized graphene sheets for polymer nanocomposites. Nature Nanotechnology. 2008;3(6):327-31.

[36]     Steurer P, Wissert R, Thomann R, Mulhaupt R. Functionalized Graphenes and Thermoplastic Nanocomposites Based upon Expanded Graphite Oxide. Macromolecular Rapid Communications. 2009;30(4-5):316-27.

[37]     Yang XM, Li LA, Shang SM, Tao XM. Synthesis and characterization of layer-aligned poly(vinyl alcohol)/graphene nanocomposites. Polymer. 2010;51(15):3431-5.

[38]     Zhao X, Zhang QH, Chen DJ, Lu P. Enhanced Mechanical Properties of Graphene-Based Poly(vinyl alcohol) Composites. Macromolecules. 2010;43(5):2357-63.

[39]     Nirmalraj PN, Lutz T, Kumar S, Duesberg GS, Boland JJ. Nanoscale Mapping of Electrical Resistivity and Connectivity in Graphene Strips and Networks. Nano Letters. 2011;11(1):16-22.

[40]     Lyons PE, De S, Blighe F, Nicolosi V, Pereira LFC, Ferreira MS, et al. The relationship between network morphology and conductivity in nanotube films. Journal of Applied Physics. 2008;104(4):

[41]     Eda G, Chhowalla M. Graphene-based Composite Thin Films for Electronics. Nano Letters. 2009;9(2):814-8.

16

[42]    Green AA, Hersam MC. Emerging Methods for Producing Monodisperse Graphene Dispersions. Journal of Physical Chemistry Letters. 2010;1(2):544-9.

[43]    Sun XM, Liu Z, Welsher K, Robinson JT, Goodwin A, Zaric S, et al. Nano-Graphene Oxide for Cellular Imaging and Drug Delivery. Nano Research. 2008;1(3):203-12.

[44]    Coleman JN, Lotya M, O'Neill A, Bergin SD, King PJ, Khan U, et al. Two-Dimensional Nanosheets Produced by Liquid Exfoliation of Layered Materials. Science. 2011;331(6017):568-71.

[45]    Duesberg GS, Burghard M, Muster J, Philipp G, Roth S. Separation of carbon nanotubes by size exclusion chromatography. Chemical Communications. 1998;(3):435-6.

[46]    Cancado LG, Jorio A, Martins Ferreira EH, Stavale F, Achete CA, Capaz RB, et al. Quantifying Defects in Graphene via Raman Spectroscopy at Different Excitation Energies. Nano Letters. 2011;dx.doi.org/10.1021/nl201432g(

[47]    De S, Coleman JN. Are There Fundamental Limitations on the Sheet Resistance and Transmittance of Thin Graphene Films? Acs Nano. 2010;4(5):2713-20.